1-2008

Analysis of Resonating Microcantilevers Operating in a Viscous Liquid Environment

Cyril Vančura
Eidgenössische Technische Hochschule

Isabelle Dufour
Université Bordeaux 1

Stephen M. Heinrich
Marquette University, stephen.heinrich@marquette.edu

Fabien Josse
Marquette University, fabien.josse@marquette.edu

Andreas Hierlemann
Eidgenössische Technische Hochschule

Sensors and Actuators A: Physical, Vol. 141, No. 1 (January 15, 2007): 43-51. DOI.

Analysis of Resonating Microcantilevers Operating in A Viscous Liquid Environment

Cyril Vančura
Physical Electronics Laboratory, Wolfgang-Pauli-Strasse 16, Eidgenössische Technische Hochschule, 8093 Zürich, Switzerland
Isabelle Dufour
IXL Laboratory, Université Bordeaux 1, ENSEIRB, CNRS UMR5818, 33405 Talence Cedex, France
Stephen M. Heinrich
Department of Civil and Environmental Engineering, Marquette University, Milwaukee, WI
Fabien Josse
Microsensor Research Laboratory, Department of Electrical and Computer Engineering, Marquette University, Milwaukee, WI
Andreas Hierlemann
Physical Electronics Laboratory, Wolfgang-Pauli-Strasse 16, Eidgenössische Technische Hochschule, 8093 Zürich, Switzerland

Abstract

The characteristics of resonant cantilevers in viscous liquids are analyzed. Various rectangular cantilevers geometries are studied in pure water, glycerol and ethanol solutions of different concentrations, and the results are described in terms of the added displaced liquid mass and the liquid damping force for both, the resonance frequency and the quality factor (Q-factor). Experimental results using a set of magnetically actuated resonant cantilevers vibrating in the out-of-plane ("weak-axis bending") mode are presented and compared to theoretical calculations. The importance of the study is in the use of resonant cantilevers as biochemical sensors in liquid environments.

Keywords

CMOS sensor, Liquid-phase operation, Resonant cantilever

1. Introduction

Several sensor technologies are being investigated for gas- or liquid-phase detection. In recent years, interest in cantilever-based chemical and bio-chemical sensing systems has risen due to their projected high sensitivity [1], [2], [3]. The large ratio of surface area-to-mass makes the microcantilever extremely sensitive to surface processes. For bio-chemical detection, the microcantilever is usually coated with a bio-chemically sensitive layer, which selectively absorbs the analyte molecules of interest. Two possible modes of operation exist: (a) the static mode and (b) the resonant mode. In the static mode, the analyte adsorption on the cantilever surface gives rise to surface stress and, thus, to a bending of the cantilever [1], [2]. In the resonant mode, the cantilever is driven at its fundamental resonance frequency (or one of the harmonic frequencies), and an increase of the cantilever mass due to analyte absorption causes a decrease of the cantilever resonance frequency [3]. In this paper, only the resonant mode will be considered. When operated in liquid environments, the mechanical properties of the fluid, i.e., density and viscosity, will influence the cantilever's dynamic behavior.

In the resonant mode of operation, an important transducer parameter is the mechanical quality factor. When operating frequency-output sensors, such as microcantilevers, in an oscillator configuration, the frequency stability and, consequently, the limit of detection (LOD) are directly dependent on the quality factor. Since bio-chemical sensors operate in either, the gas or the liquid phase, the quality factor of the resonant microcantilever is not as high as that of microcantilevers operating in vacuum [4]. When a microcantilever is placed in a gas atmosphere, the resonance frequency is usually reduced by a few percent or less, whereas the quality factor is decreased by orders of magnitude with respect to its value in vacuum [5]. The immersion of the cantilever in a liquid results in even more pronounced changes in the frequency response with the quality factor being another order of magnitude lower in comparison to the gas phase. The reduced value of the quality factor is due to energy dissipation in the surrounding medium and directly affects the sensitivity and detection limit of this type of sensor.

The aim of this paper is to study the out-of-plane vibration mode (for various rectangular cantilever geometries), which is the most commonly used mode in cantilever research. This mode relies on the out-of-plane bending of the cantilever, for which the flexural stiffness is minimal (Fig. 1a). Another vibration mode is the in-plane vibration mode (Fig. 1b). The advantages of this mode are minimized dissipation losses to the surrounding fluid and maximized flexural stiffness. A consequence of the high flexural stiffness is that this mode is very difficult to excite. We therefore limit ourselves to the out-of-plane vibration mode.

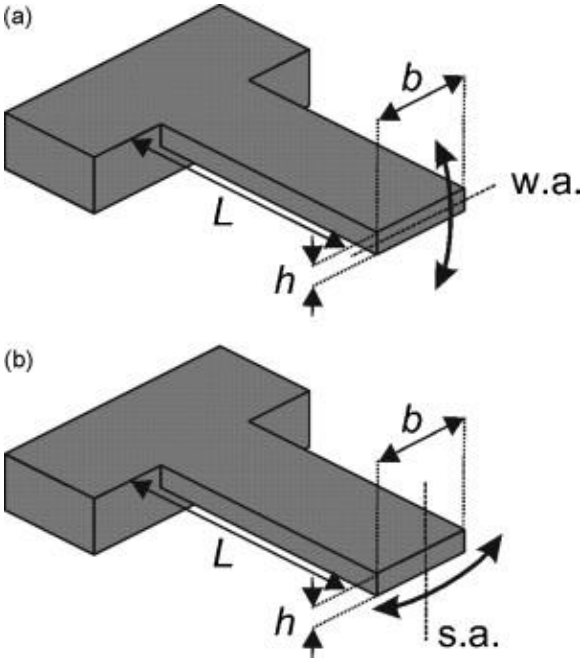

Fig. 1. (a) Out-of-plane bending. (b) In-plane bending mode of vibration (w.a. and s.a. denote the “weak” and “strong” axis of the cantilever).

In the first part of the paper, relevant theoretical results are presented for microcantilever beam vibrations. These results include equations for the resonance frequency, the forces associated with the surrounding fluid, the quality factor, and the frequency shift caused by an added mass on the beam surface based on a lumped-element model. In the experimental part of this paper, measurements of various cantilevers vibrating in viscous fluids featuring different viscosities are compared with theoretical results. These measurements have been performed with magnetically actuated microcantilevers, fabricated in CMOS technology with post-CMOS micromachining. As will be shown, the sensor dynamics in the liquid are strongly dependent on the cantilever width.

2. Microcantilever mechanics

2.1. Fluid losses, resonance frequency and quality factor

When a microcantilever vibrates in a viscous fluid, the fluid offers resistance to the motion of the beam, which can be described by an external force acting on the cantilever [6]. This force can be expressed in two terms. The first term is a dissipative force per unit length, which results from the fact that the motion of the fluid is not necessarily in phase with the cantilever motion. It is called the fluid damping force and is proportional to the cantilever velocity. The second term is proportional to the cantilever acceleration and results from the fluid being forced into motion with the cantilever. This term is due to the inertia of the fluid mass displaced by the motion of the cantilever. Combining these two terms, the total fluid force, F_{fluid}, per unit length of the cantilever can be written as [6]:

(1) $$F_{\text{fluid}} = -g_1\dot{w} - g_2\ddot{w}$$

is the deflection at an arbitrary location, x, on the beam axis. In Eq. (1), g_1 is the fluid damping coefficient and g_2 is the added fluid mass per unit length of the beam. More details on these two factors will be given later in this paper.

Using the expression of the fluid force given in Eq. (1), the resonance frequency, f_r, of the microcantilever immersed in a viscous fluid can be related to its undamped natural frequency in vacuum, f_0 [7]:

(2) $$f_r = f_0 \frac{1}{\sqrt{1+\frac{Lg_2}{m}}} \sqrt{1 - \frac{1}{2Q_{tot(liq)}^2}}$$

with L being the cantilever length and m representing the cantilever mass. $Q_{tot(liq)}$ is the quality factor of the immersed cantilever taking into account all losses in the fluid as well as the intrinsic losses in the microstructure. It should be noted that the term “natural frequency” is used to denote the frequency, at which a free, unforced vibration may occur, whereas the term “resonance frequency” refers to the maximum-amplitude frequency of a forced vibration. Under identical environmental conditions, the resonance frequency is always smaller than the natural frequency due to internal losses in the cantilever structure.

For a composite cantilever, such as a CMOS cantilever used in the experiments performed in this work, the undamped natural frequency, f_0, can be expressed as follows:

(3) $$f_0 = \frac{1}{2\pi} \left(\frac{\lambda_0}{L}\right)^2 \sqrt{\frac{\sum_i \hat{E}_i I_i}{b \sum_i \rho_i h_i}}$$

with $\lambda_0 = 1.875$ denoting the fundamental flexural mode and b being the cantilever width. Eq. (3) is derived from the classical beam bending theory. The parameters ρ_i and h_i are the density and thickness of the respective layers of the composite cantilever. I_i represents the individual moments of inertia of the different layers with respect to the neutral axis of the beam. The apparent Young's moduli of the respective cantilever layers are denoted $\hat{E}_i$.

The quality factor, $Q_{tot(liq)}$, of a liquid-immersed microstructure takes into account the fluid damping as well as internal damping effects caused by, e.g., support losses. Expressing the quality factor as the sum of its two main components yields:

(4) $$\frac{1}{Q_{tot(liq)}} = \frac{1}{Q_{int}} + \frac{1}{Q_{fluid}}$$

fluidwith Q_{int} being the intrinsic quality factor of the microstructure and Q_{fluid} the fluid contribution to the quality factor, i.e., the fluid-induced losses in the liquid. As will be shown in the experimental section, the fluid-induced losses tend to dominate, when the resonant microcantilever is operated in the out-of-plane mode in a viscous liquid, such as water. It is therefore possible to neglect the contribution of the intrinsic losses, and to replace the overall quality factor in Eq. (2) by the fluid-dependent quality factor ($Q_{tot(liq)} \approx Q_{fluid}$). Q_{fluid} is a function of the two fluid coefficients g_1 and g_2, which, in turn, are functions of the frequency, f_r. Using the results of Sader [6], the fluid-dependent quality factor can be written as

(5) $$Q_{fluid} = 2\pi f_0 \frac{\sqrt{1+Lg_2/m}}{Lg_1/m}$$

which takes into account losses as a consequence of the liquid-phase environment. The fluid coefficients, g_1 and g_2 in Eq. (5) are given by

(6) $$g_1 = \pi \eta Re \Gamma_i(Re)$$

(7) $$g_2 = \frac{\eta Re}{2f_r} \Gamma_r(Re)$$

is the fluid viscosity and Re is the Reynolds number of the liquid flow around the cantilever. Γ_r and Γ_i are the real and imaginary parts of the “hydrodynamic function”:

(8) $$\Gamma(Re) = \Omega(Re)\left[1 + \frac{4\mathrm{j}K_1\left(-\mathrm{j}\sqrt{\mathrm{j}Re}\right)}{\sqrt{\mathrm{j}Re}K_0\left(-\mathrm{j}\sqrt{\mathrm{j}Re}\right)}\right]$$

with the Reynolds number, Re, of a beam vibrating at a frequency, f_r, in a fluid of density, ρ_f, being defined as

(9) $$Re = \frac{\pi\rho_f b^2 f_r}{2\eta}$$

As can be seen, the Reynolds number scales with the square of the cantilever width. In Eq. (8), K_0 and K_1 are modified Bessel functions and $\Omega(Re)$ is a correction function associated with the rectangular beam cross-section. Eq. (8) has been derived for long and slender beams, i.e., the beam length is assumed to be much larger than the beam width. Furthermore, it should be noted that the Reynolds number is, according to Eq. (9), proportional to the oscillation frequency, which represents the unknown parameter to be calculated here. Thus, it is necessary to perform a self-consistent calculation of the resonance frequency, f_r. This is done by first calculating the Reynolds number according to Eq. (9) with the resonance frequency in air as starting value. The value of the Reynolds number is then used to calculate the value of g_1 and g_2 according to Eqs. (6), (7). These calculated values can be used to obtain the new resonance frequency in liquid according to Eq. (2) and the new Reynolds number according to Eq. (9). This iterative process is continued until self-consistency is reached. Four iteration steps were found to be sufficient in this study. For the calculation of the resonance frequencies in different ethanol/water or glycerol/water mixtures, the calculated resonance frequency at the respective lower additive concentration was chosen as a starting value for the iteration of the next step of higher concentration.

3. Cantilever system and packaging

The liquid-phase measurements to be presented here have been performed with an integrated CMOS (complementary metal oxide semiconductor) microcantilever system that includes an array of four cantilevers and the necessary readout and signal conditioning circuitry on the same chip. The system is fabricated in an industrial 0.8-µm CMOS process combined with post-CMOS micromachining, during which the multilayer cantilevers (silicon, silicon oxide and silicon nitride) have been formed by means of etching processes.
The fabrication process is described in more detail in [8]. The cantilevers are 8.2 µm thick and consist of a single-crystal silicon (5.0 µm) layer and the two dielectric layers of the CMOS process on top (2.2 µm silicon oxide and 1 µm silicon nitride). Owing to the negligible out-of-plane curvature of the used cantilevers it is possible to model them as initially flat plates. Electromagnetic actuation based on the presence of a static, external magnetic field and the generation of Lorentz forces was used to drive the various cantilevers. The cantilevers featured a length of 200 µm and widths between 50 µm and 186 µm. A current in the metal path along the edges of the cantilever, which has been realized using the two metal layers of the CMOS process, gives rise to the Lorentz forces. If the magnetic field, B, is oriented in parallel to the cantilever axis, the Lorentz force, F_L, is oriented perpendicularly to the cantilever plane. The arrangement of magnetic field, current and Lorentz force is shown in Fig. 2a. The Lorentz force acts on the cantilever tip, where the current and the magnetic field are perpendicular to each other. By applying a sinusoidal current, an out-of-plane cantilever oscillation can be achieved. This oscillation is read out by a Wheatstone bridge composed of four stress-sensitive PMOS transistors, integrated near the clamped edge of the cantilever.

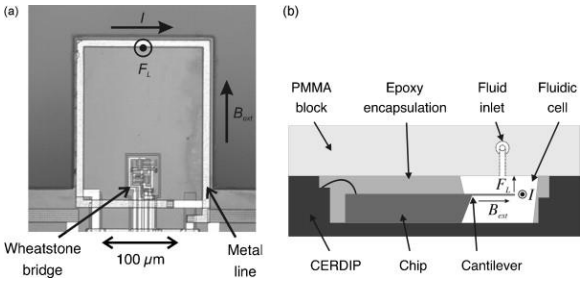

Fig. 2. (a) Micrograph of a resonant cantilever featuring an integrated, stress-sensitive transistor Wheatstone bridge for read out and a current loop for electromagnetic actuation. The directions of the current *I*, the external magnetic field, B_{ext}, and the Lorentz force, F_L, are indicated. (b) Cross-sectional schematic of the packaged cantilever chip [12]. The direction of the current, *I*, at the cantilever tip is indicated (CERDIP stands for ceramic dual-in-line package).

The packaging of the cantilever chip must meet the following two requirements: (a) all electrical connections as well as the integrated circuitry must be protected against contact with the conducting fluids; (b) a fluidic cell must be fabricated that hosts the cantilevers and enables liquid handling. The diced chip has been mounted on a standard ceramic dual-in-line-package (CERDIP) and has been electrically connected via wire bonding. The bond wires and the integrated electronics have been protected with UV-curable epoxy (OG116, Epoxy Technology, Inc., Billerica, MA, USA) in order to avoid short-circuits. Due to its high viscosity, the epoxy can be applied without any risk of accidental coverage of the cantilevers. The epoxy is also used to form the fluidic cell accommodating the cantilevers by placing a mold in the CERDIP before dispensing the epoxy. The fluidic cell is closed by a machined plexiglass block with inlet and outlet for the liquid. A schematic view of the packaged cantilever chip can be seen in Fig. 2b, where only the vibrating cantilever is exposed to the fluid. The actuation and readout circuitry on the cantilever is protected by the passivation nitride of the CMOS process, which turned out to be pin hole free and sufficiently protective for reliable operation. The packaged chip with the fluidic cell is mounted onto a printed-circuit board (PCB) and placed in a tunable electromagnet, which provides the magnetic field for the cantilever actuation. After filling the fluidic cell with a particular liquid, the cantilever characteristics are measured by means of an HP 4194A gain-phase analyzer.

4. Results and discussion

First, the effect of the actuation amplitude was studied by increasing the magnitude of the magnetic field with the tunable electromagnet from 50 mT to 250 mT. These measurements were done with a test cantilever featuring a length of 150 μm, a width of 140 μm, and a thickness of 8.2 μm. It is noted that small discrepancies will exist between theory and experiments as the theory strictly holds only for long and slender cantilevers, whereas some of the measurements were done with almost square-shaped cantilevers. However, the results from beam theory can still be applied to the analysis of the square beams [9]. From cantilever beam theory, the resonance frequency of a damped cantilever is determined by the mechanical properties of the cantilever, such as its stiffness and mass, and by the damping [10]. As expected, the measured resonance frequency was independent of the actuation amplitude. However, a slight increase in the *Q*-factor of less than 3% was measured when doubling the magnetic field strength. This is due to an improved signal extraction, as the signal-to-noise ratio increases with increasing magnetic field strength. As expected, the output voltage, which is proportional to the vibration amplitude, is correlated to the magnitude of the external magnetic field, rising from 0.9 mV at 100 mT to 1.8 mV at 200 mT for a 200 mV input voltage. The peak-to-peak noise amplitude is independent of the magnetic field strength and is below 0.02 mV. These measurements suggest that the operating point for further characterization can be freely chosen in the investigated range because the measurement data are fairly independent of the magnetic field strength. A high magnetic field is favorable in

order to increase the signal-to-noise ratio. Therefore, the cantilever characterizations have been conducted at an external magnetic field of B_{ext} = 200 mT.

In order to validate the theoretical approach presented in Section 2, the measurements conducted with different cantilever geometries presented in Section 3 have been compared to the theoretical predictions. The measurements of the quality factor in air, $Q_{tot(air)}$, and liquid, $Q_{tot(liq)}$, show that $Q_{tot(air)}$ is much larger than $Q_{tot(liq)}$ (i.e., $Q_{tot(air)} \gg Q_{tot(liq)}$), which indicates that the value of the quality factor in liquids is dominated by the viscous losses for all four cantilever geometries.

Fig. 3 shows the comparison of the amplitude spectrum of a cantilever of 200 µm length and 140 µm width in air and in a glycerol/water mixture (10% glycerol mass fraction). The resonance frequency of the cantilever in air is 206.5 kHz and 93.4 kHz in water. Furthermore, a quality factor of 900 in air is reduced to 17 in the liquid phase. These values were extracted from the measured amplitude spectra by least-mean-squares fitting of a Lorentzian peak and have an uncertainty of about 5%. From Eq. (2), it can be concluded that the shift in the resonance frequency is a consequence of the added mass term (Lg_2/m). The effect of the reduced quality factor (see Eq. (2)) only would account for a drop of less than 0.2% of the resonance frequency. Consequently, the observed frequency drop of 55% has to be caused by the increase of the equivalent cantilever mass. In the liquid, the cantilever drags along a specific volume of liquid during movements; hence, the cantilever behaves as if its mass were much larger than it really is. Table 1 summarizes the fluid damping term (Lg_1/m) and the added mass term (Lg_2/m) in water for the four different cantilever geometries. As can be seen, the two terms show opposite trends with respect to the cantilever width. With increasing cantilever width the added mass increases, whereas the damping term is reduced. The tabular values of (Lg_2/m) indicate that a larger percentage of equivalent fluid mass (relative to beam mass) is being displaced as the cantilever width increases, which indicates that a wider cantilever seems to act more like a paddle, whereas, in the case of a narrow cantilever, the fluid tends to flow around the cantilever. An opposite trend is observed in the width-dependence of (Lg_1/m). The values demonstrate that the ratio of the fluid dissipative force (Lg_1) to beam mass, m, decreases as beam width increases. This may be explained by the fact that beam mass is proportional to width, but one would expect the viscous forces to be more dependent on beam thickness (a parameter that is held constant in Table 1) rather than beam width.

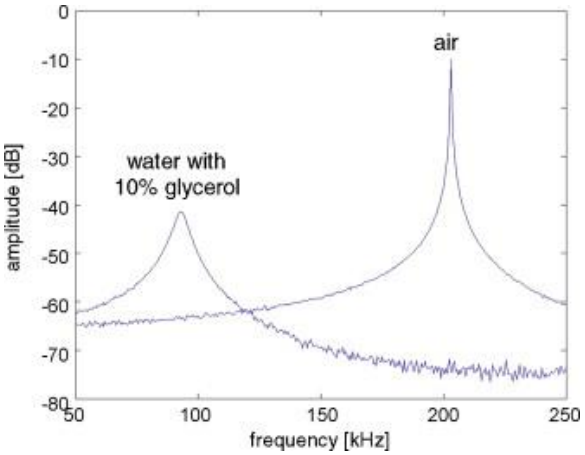

Fig. 3. Measured spectra of a cantilever of 200 µm length, 140 µm width and 8.2 µm thickness in air and in a glycerol–water mixture.

Table 1. Measured dissipative terms and mass terms of the fluid damping force and comparison to their theoretical predictions in water for different cantilever geometries of 200 µm length, 8.2 µm thickness and variable widths

Cantilever width (µm)	**(Lg_1/m) (×10^3 Hz)**	**(Lg_2/m)**	**$(Lg_1/m)_{theo}/(Lg_1/m)_{meas}$**	**$(Lg_2/m)_{theo}/(Lg_2/m)_{meas}$**

50	229	2.1	0.97	1.01
100	186	2.8	1.03	1.34
140	179	3.5	0.97	1.39
186	162	4.2	1.00	1.47

Table 1 also shows the ratios of the measured values and the theoretical predictions of the dissipative and the mass terms for all four-cantilever geometries. The theoretical predictions are based on using Eqs. (2), (5) to calculate values corresponding to measured values of resonance frequency and quality factor. As can be seen, the dissipative term is predicted very well, with a discrepancy between measurements and theory of less than 3% in all cases. The mass term (Lg_2/m), on the other hand, is correctly predicted only in the case of the narrow cantilever with a width of 50 µm. For this case the cantilever aspect ratio, which is defined as the ratio of the cantilever length, L, to the cantilever width, b, is $L/b = 4$. For the cantilevers with lower aspect ratios the deviation of the theory from the measured values increases with decreasing aspect ratio. For the widest cantilever (186 µm width) the deviation is 47%. This observation is consistent with data on the characteristics of cantilevers with aspect ratios larger than 4 operated in different fluids [5], [11]. The reason for the deviation between the measured and predicted values for the wide cantilevers is that Eq. (8) is derived under the assumption that L is much larger than b. This is certainly not the case for the cantilevers used in this study, where L and b are of similar magnitude. Hence, the amount of fluid that is moving in phase with the cantilever is overestimated by the model. As a consequence of the overestimation in the added mass term, the resonance frequency calculated according to Eq. (2) is much lower than the measured value. From Table 1 it is also possible to calculate the apparent height of the fluid column, with its cross-section matching the area of the cantilever, vibrating with the same magnitude as the cantilever. The calculated values are 40 µm, 53 µm, 67 µm and 80 µm for the four different cantilever designs featuring widths of 50 µm, 100 µm, 140 µm and 186 µm, respectively. Comparing these values to the lateral distance of the cantilever surfaces to the respective walls of the fluid cell (∼400 µm underneath the cantilever and ∼500 µm above cantilever) indicates that squeezed-film damping does not contribute to the damping of the cantilever. The comparison between the measured and the predicted resonance frequencies in water is shown in Table 2.

Table 2. Measured resonance frequencies in air and water and calculated resonance frequencies in water for four different cantilever geometries of 200 µm length, 8.2 µm thickness and variable widths.

Cantilever width (µm)	$f_{\text{meas}}^{\text{air}}$ **(kHz)**	$f_{\text{meas}}^{\text{water}}$ **(kHz)**	$f_{\text{theo}}^{\text{water}}$ **(kHz)**	$f_{\text{theo}}^{\text{water}} / f_{\text{meas}}^{\text{water}}$
50	285.6	165.9	161.1	0.97
100	274.1	142.2	125.7	0.88
140	266.4	129.7	109.9	0.85
186	261.9	120.5	97.7	0.81

To demonstrate the frequency behavior of the different cantilever geometries at low glycerol concentrations in water (see also [12]), Fig. 4a depicts frequency measurements of three different cantilevers in glycerol–water mixtures with glycerol mass fractions up to 16% at room temperature. The frequency shift with respect to the resonance frequency in pure water is plotted versus the kinematic viscosity, ν, of the solution, which is defined as the ratio of its viscosity and density ($\nu = \eta/\rho_f$). As reference point the kinematic viscosities of water (ν = 1 cS), glycerol (ν = 1189 cS), and ethanol (ν = 1.5) are given at a temperature of 20 °C. It should be noted that all measurements have been conducted at room temperature. At low glycerol concentrations (as depicted in Fig. 4a) the change in density and viscosity is approximately linear. The slight curvature of the measurement data plot results on the the nonlinear dependence of the frequency from kinematic viscosity, which is in good

agreement with theoretical calculations [6]. Fig. 4b shows a typical measurement of the frequency behavior of the narrow cantilever (L = 200 µm and W = 50 µm) in glycerol–water mixtures with increasing glycerol mass fractions up to 60%. In this concentration range, the density of the mixture shows an approximately linear increase of about 14%, whereas the viscosity shows a strong, nonlinear increase by one order of magnitude [13]. As can be seen, the frequency shift is correctly predicted by the theoretical calculations, which are represented by the solid line. The deviation between the measurements and the calculations is less than 8% for all concentration steps. For other cantilever geometries with lower aspect ratios, the discrepancy between the measured and calculated frequency shifts is much larger (up to 25%). This is due to the initial discrepancy between the measured and the calculated resonance frequency in water, which leads to a larger frequency shift in the calculation for the glycerol–water solutions. Fig. 5 shows the frequency shifts of two selected cantilever geometries immersed in different glycerol water mixtures. The values of frequency shift have been normalized with respect to the corresponding resonance frequencies in water. The results show a good agreement between the measurements and the calculated values over the entire concentration range for both cantilever geometries. Hence, by normalizing the frequency shifts with respect to the initial resonance frequency in water, the effect of the underestimation of the resonance frequency in water can be eliminated.

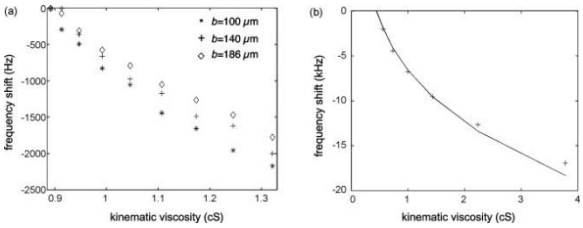

Fig. 4. (a) Measured frequency shifts of three cantilevers featuring a length of L = 200 µm and different widths, b, that have been immersed in glycerol–water mixtures with low glycerol mass fractions up to 16% [12]. The glycerol content was increased from 0% (pure water) to 16% in steps of 2%. The data are plotted versus the kinematic viscosity, defined as the ratio of the fluid viscosity and density. (b) Measured and predicted frequency shift of a cantilever of 200 µm length and 50 µm width immersed in different glycerol–water mixtures with mass fractions up to 60% (+: measured values, −: predicted values). The glycerol content was increased from 0% (pure water) to 60% in steps of 10%.

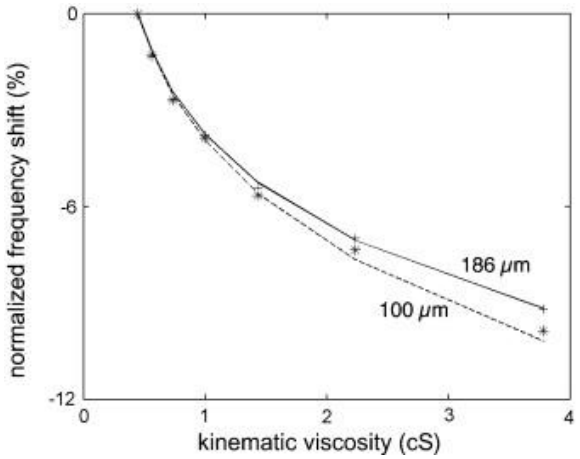

Fig. 5. Normalized frequency shift of two cantilevers of 200 µm length and 100 µm and 186 µm width that have been immersed in different glycerol–water mixtures with increasing glycerol mass fractions up to 60%. Solid and dashed lines represent the theoretical predictions for the respective cantilever widths. The glycerol content was increased from 0% (pure water) to 60% in steps of 10%.

The results for the quality factor of the narrow cantilever featuring a width of 50 µm (Fig. 6) show good agreement between the measurements and the calculated values according to Eq. (5). The results for the

cantilevers in ethanol solutions (Fig. 6a) show that the quality factor decreases with increasing ethanol concentration. Similar trends have been obtained for the other cantilever geometries (not plotted), and again, the wider cantilevers show a significant discrepancy between the measured values and the calculated values, a deviation which increases with increasing cantilever width. This is a result of the overestimation in the mass term (Lg_2/m). According to Eq. (5), the overestimated mass term leads to a too large quality factor. To reflect the quality factor behavior of the different cantilever geometries at low glycerol contents in water (see Ref. [12]), Fig. 6b depicts the quality factors of four different cantilevers in glycerol–water mixtures with glycerol concentrations up to 16%. All four cantilevers show a decrease of the Q-factor with increasing glycerol content in the mixture. This decrease cannot be explained by only taking into account the increasing equivalent mass of the cantilever as a consequence of the additional glycerol in the mixture. This holds in particular since, according to Eq. (5), an increasing equivalent mass will result in an increase of the quality factor. Thus, the decrease has to be attributed to the increasing damping of the cantilever, which overcompensates for the effect of the increasing effective cantilever mass.

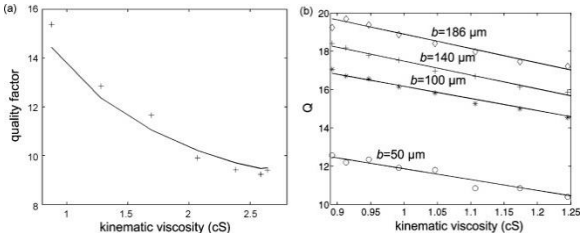

Fig. 6. (a) Quality factor change of a cantilever of 200 µm length and 50 µm width immersed in ethanol–water mixtures with increasing ethanol content (+: measured values, −: predicted values). The ethanol content was increased from 0% (pure water) to 60% in steps of 10%. (b) Measured quality factors of four cantilevers of 200 µm length and different widths, b, immersed in glycerol–water mixtures of low glycerol content up to 16% [12]. The glycerol content was increased from 0% (pure water) to 16% in steps of 2%.

Fig. 7 shows the measured quality factors of four cantilevers of different widths as a function of the ethanol content in the solution over the whole concentration range from pure water to pure ethanol. The kinematic viscosity shows a maximum at approximately 60% ethanol content owing to the strong nonlinear behavior of the viscosity of ethanol–water mixtures [13]. As a consequence, the quality factors of the different cantilevers show a minimum at about 60% ethanol content as can be seen in Fig. 7. Moreover, it can be seen that the quality factor increases with increasing cantilever width. This behavior can be explained by the following consideration. If the obstructions to fluid motion are far enough away, a column of fluid above and underneath the rectangular cantilever is pushed and pulled in phase with the cantilever motion, with only small gradients in the velocity field. As has been already mentioned the height of the apparent fluid column is significantly smaller than the distance between the cantilever surfaces and the walls of the fluid cell. As a consequence squeezed-film damping does not have to be taken into account. Around the three moving edges of the cantilever, in a boundary layer, more significant gradients in the velocity field magnitude and phase do occur. Outside this fluid column and the adjacent boundary layer the fluid does not move much. The column will be widening with increasing distance to the cantilever (i.e., a quasi conical column), with the average magnitude of the velocity field in the column decreasing with increasing distance to the cantilever. The apparent inertia of the fluid can be considered as the mass of an apparent prismatic fluid column, i.e., a column with constant cross-sectional area, with its base matching the cantilever area, and with an apparent height. Hence the apparent inertia of the fluid will roughly be proportional to the cantilever width and length. In contrast, the apparent resistance of the fluid against motion is related to the real part of the gradients in the velocity field around the cantilever. The apparent damping is proportional to the sum of twice the weighted length of the cantilever (for the gradients along the sides of the cantilever) and the width of the cantilever (for the gradient along the free edge of the cantilever). Hence, the apparent damping is to a lesser extent a function of the cantilever length and width in

comparison to the apparent inertia. According to Eq. (5) an increase of the quality factor with increasing cantilever width results.

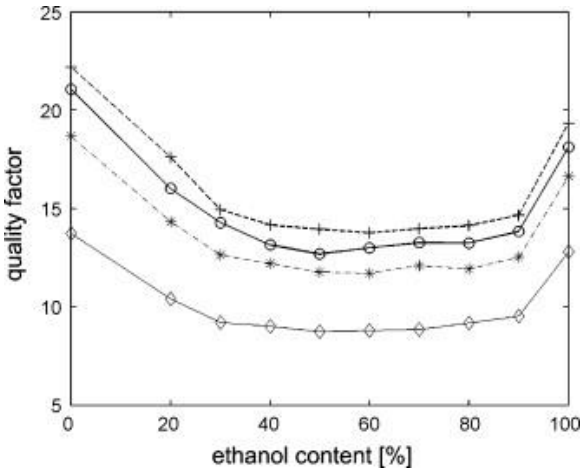

Fig. 7. Quality factors of four different cantilever geometries of 200 µm length, 8.2 µm thickness and widths between 50 µm and 186 µm as a function of the ethanol concentration in the water–ethanol mixture. Cantilever widths (+) 186 µm, (○) 140 µm, (*) 100 µm and (◊) 50 µm.

From Table 1 it is possible to calculate the apparent damping force (Lg_1) by multiplying the results from column two by the mass of the respective cantilever (Table 3). As a result, it can be seen that Lg_1 scales linearly with the cantilever width. The zero point offset in this result is due to the damping force along the two sides of the cantilever, each with a length of 200 µm, weighted with a factor less than unity owing to the mode shape of the cantilever vibration. Also the height of the apparent water column scales linearly with the cantilever width as it is summarized in Table 3.

Table 3. Value of absolute damping coefficient, Lg_1, and height of apparent water column, t_{water}, forced into motion by the cantilever for four different cantilevers of 200 µm length, 8.2 µm thickness and different widths

Cantilever width (µm)	$\boldsymbol{Lg_1}$ **(×10^{-6} kg/s)**	$\boldsymbol{t_{water}}$ **(µm)**
50	44	40
100	71	53
140	96	67
186	115	80

As indicated, the importance of this study is in the use of resonant cantilevers as biochemical sensors in viscous fluid environments. The cantilever discussed in the previous sections can indeed be used as mass sensitive devices by coating them with chemically or biologically sensitive layers. When such a cantilever is placed in a gas or liquid environment containing analyte molecules, a fraction of the analyte molecules will be absorbed by or adsorbed onto the sensitive layer or receptor structure. Hence, the physical properties of the sensitive layer will change, which, in turn, will lead to a change in the cantilever mass, stiffness, and/or damping. The resulting frequency shift in the cantilever resonance frequency can be expressed in terms of mass variation, stiffness variation, etc. In practice, it was observed that the frequency shift is dominated by the mass variation of the sensitive layer in the case of polymer-coated microcantilevers [14]. Assuming the analyte-induced damping and stiffness variations to be negligible (low analyte concentrations), the frequency shift is due entirely to the mass increase, Δm, of the sensitive layer and can be written as

(10) $\Delta f_{\mathrm{r}} = -\frac{f_{\mathrm{r}}}{2}\frac{1}{1+Lg_2/m}\frac{\Delta m}{m}$

It is worth mentioning that *m* corresponds to the total mass of the cantilever including that of the sensitive layer in this notation. Using Eq. (2), the frequency shift can be rewritten as

(11) $\Delta f_{\mathrm{r}} = \frac{f_0}{2}\frac{1}{\left(1+\frac{Lg_2}{m}\right)^{3/2}}\sqrt{1-\frac{1}{2Q^2_{\mathrm{tot(liq)}}}}\frac{\Delta m}{m}$

The presented results indicate that the term representing the inertial drag force (Lg_2/m) can be neglected in the gas phase because the inertial effect of the air on the cantilever response is very small. However, in a liquid medium, this term is significant and has to be included.

Eq. (11) indicates that the mass sensitivity of a cantilever can be enhanced by increasing the natural frequency (e.g., by increasing the bending stiffness or decreasing beam mass), by increasing the quality factor, or by decreasing the added fluid mass (Lg_2), forced into motion by the cantilever. However, as the *Q*-factor of the cantilevers is more than 10 even in liquid environments, an increase of the quality factor does not significantly enhance the cantilever sensitivity. The contributions of the resonance frequency and the added fluid mass, the latter of which is included in the $(1 + Lg_2/m)^{3/2}$ factor in the denominator, are more important. As mentioned in the introduction the interesting figure of merit of such a cantilever sensing system operated as frequency determining element in an oscillator loop is the minimum detectable mass change. This value is dependent on the sensitivity and the overall frequency stability of the system. Measured values of the frequency stability and the limit of detection of a cantilever sensing system similar to the one presented in this paper have been shown in [8].

One way to overcome or significantly reduce the liquid damping and the effect of the added mass is to actuate the cantilever in an in-plane or torsional mode instead of the out-of-plane mode described in this paper. Theory predicts that these modes show lower viscous losses and smaller equivalent fluid mass being forced into motion along with the microcantilever [7]. These advantages would result in an improved mass sensitivity of the devices in liquid environments. The implementation of in-plane mode vibrations of a cantilever beam is more difficult than the implementation of out-of-plane mode vibrations. A possible realization of an integrated in-plane mode actuation for a cantilever beam may be a thermal actuation with two integrated heaters at the clamped edge of the cantilever. Another possibility is the magnetic actuation in an inhomogeneous magnetic field generated by two conductor lines in close proximity to the cantilever. In that case a dc current is driven through two conductor lines on the chip substrate parallel to the cantilever. The magnetic field generated by these two currents is such that an oscillating current through the metal path on the cantilever would cause an oscillating Lorentz force in the cantilever plane. This is similar to the actuation concept that has been presented in [15]. As the Lorentz force is expected to be small, this actuation scheme would require small gaps between the substrate and the cantilever. Furthermore, a reduction of the cantilever width at the suspension will most probably be necessary (paddle-shaped cantilever) in order to provide a detectable vibration amplitude. Such a width reduction at the suspension, however, will result in a reduction of the cantilever stiffness or lead to the excitation of torsional cantilever modes. The electromagnetic actuation of a torsional mode has been presented in Ref. [16].

5. Summary and conclusions

The modeling results for resonance frequency and quality factor of out-of-plane mode cantilevers have been compared to measurements performed with a set of CMOS-based microcantilevers. The cantilevers have been immersed in water and glycerol or ethanol solutions and have been characterized with regard to the geometrical dimensions of the cantilever and the liquid properties. When immersed in a fluid, the equivalent mass of the cantilever increases and the viscous damping becomes important. The measured cantilever resonance frequencies and quality factors show good agreement with the values extracted from the presented lumped-element model. The model indicates that the mass sensitivity of a cantilever can be enhanced by increasing the natural frequency (e.g., by increasing the bending stiffness or decreasing beam mass), increasing the quality factor, or by decreasing the added fluid mass forced into motion by the cantilever. This can be achieved for example by operating a cantilever in an in-plane mode instead of the out-of-plane mode presented here.

Acknowledgements

The authors acknowledge Prof. Henry Baltes for his stimulating interest in their work. This work has been funded by the Swiss Federal Office of Science and Education within the EU project “Biofinger” (IST-2001-34544).

References

[1] R. McKendry, J. Zhang, Y. Arntz, T. Strunz, M. Hegner, H.-P. Lang, M.K. Baller, U. Certa, E. Meyer, H.-J. Güntherodt, C. Gerber. **Multiple label-free biodetection and quantitative DNA-binding assays on a nanomechanical cantilever array.** *PNAS*, 99 (2002), p. 9783

[2] M. Calleja, J. Tamayo, A. Johansson, P. Rasmussen, L. Lechuga, A. Boisen. **Polymeric cantilever arrays for biosensing applications.** *Sens Lett.,* 1 (2004), p. 1

[3] M. Sepaniak, P. Datskos, N. Lavrik, C. Tipple. **Microcantilever transducers: a new approach in sensor technology.** *Anal. Chem*., 74 (21) (2002), p. 569A

[4] F.R. Blom, S. Bouwstra, M. Elwenspoek, J.H.J. Fluitman. **Dependence of the quality factor of micromachined silicon beam resonators on pressure and geometry.** *J. Vac. Sci. Technol. B*, 10 (1992), p. 19

[5] J.W.M. Chon, P. Mulvaney, J.E. Sader. **Experimental validation of theoretical models for the frequency response of atomic force microscope cantilever beams immersed in fluids.** *J. Appl. Phys*., 87 (2000), p. 3978

[6] J.E. Sader. **Frequency response of cantilever beams immersed in viscous fluids with applications to the atomic force microscope.** *J. Appl. Phys*., 87 (1998), p. 64

[7] I. Dufour, S.M. Heinrich, F. Josse, Strong-axis bending mode vibrations for resonant microcantilever (bio)chemical sensors in gas or liquid phase, Pr*oceedings of the 2004 IEEE International, Montreal, August 23–27, 2004.*

[8] C. Vancura, Y. Li, J. Lichtenberg, K.-U. Kirstein, A. Hierlemann, F. Josse. **Liquid-phase chemical and biochemical detection using fully integrated magnetically actuated complementary metal oxide semiconductor resonant cantilever sensor systems.** *Anal. Chem*., 79 (4) (2007), p. 1646

[9] D. Paci, K.-U. Kirstein, C. Vancura, J. Lichtenberg, H. Baltes. **A behavioural model of resonant cantilevers for chemical sensing.** *Analog Integr. Circuits Signal Process*., 44 (2005), p. 119

[10] W. Weaver, S.P. Timoshenko, D.H. Young. ***Vibration Problems in Engineering.*** Wiley, New York (1990)

[11] S. Kirstein, M. Mertesdorf, M. Schönhoff. **The influence of a viscous fluid on the vibration dynamics of scanning near-field optical microscopy fiber probes and atomic force microscopy cantilevers.** *J. Appl. Phys*., 84 (1998), p. 1782

[12] C. Vančura, J. Lichtenberg, F. Josse, A. Hierlemann. **Characterization of magnetically actuated resonant cantilevers in viscous fluids.** *Appl. Phys. Lett*., 87 (2005), p. 162510

[13] N.E. Dorsley. ***Properties of Ordinary Water-Substances.*** Reinhold, New York (1940)

[14] U. Sampath, S.M. Heinrich, F. Josse, F. Lochon, I. Dufour, D. Rebière. **Study of viscoelastic effect on the frequency shift of microcantilever chemical sensors.** *IEEE Trans. Ultrason. Ferroelectr. Freq. Contr., 53 (11) (2006)*, p. 2166

[15] J.H. Seo, O. Brand. **Self-magnetic excitation for in-plane mode resonant microsensors.** *Tech. Digest IEEE MEMS'06, Istanbul, January 22–26 (2006)*, p. 74

[16] D. Jin, X. Li, Z. Zhang, H. Bao, Y. Wang, J. Liu, H. Yu, Integrated resonant cantilever sensors with second torsion-mode for fg-level resoluble biomedical detection, *Tech. Digest IEEE MEMS'07, Kobe, January 21–25, 2007*, p. 1137.